Paramagnetic Bimetallomesogens†

J. Barberá, R. Giménez, M. Marcos, J. L. Serrano,* P.J. Alonso, and J. I. Martínez

Instituto de Ciencia de Materiales de Aragón, Facultad de Ciencias, Universidad de Zaragoza-CSIC, 50009 Zaragoza, Spain

Received October 3, 2002. Revised Manuscript Received December 18, 2002

The synthesis, characterization, and mesomorphic properties of copper(II) and vanadyl-(IV) complexes derived from mono-, di-, or tridecyloxy-4-benzoyloxysalicylidene-3,3′-diaminobenzidine are reported. These bimetallic complexes and the respective ligands exhibit columnar hexagonal mesomorphism when they possess 8 or 12 terminal chains and smectic C mesomorphism is displayed for compounds with 4 terminal chains, as was determined by means of optical microscopic and X-ray analysis. The complexes were paramagnetic and they were studied by EPR. The differences in molecular packing between calamitic and columnar complexes are shown clearly from comparison of the measured EPR spectra. The thermal evolution of a parameter that reflects the order of the molecules within each column of the mesophase for a columnar vanadyl complex was obtained.

Introduction

Soon after some metal-containing compounds appeared as mesogenic structures, researchers in the field of liquid crystals envisioned the interesting posibilities of these complexes.[1] One of the aspects that makes them different from typical organic liquid crystals is the rich variety of molecular geometries that can be obtained by introducing metals into the chemical structures.

Metallomesogens are especially important since materials of this type promise to expand the range of technological applications and physical properties exhibited by traditional liquid crystals due to the rich electronic states inherent in the metal centers.[2]

The development of bimetallic mesogens is an important step in the field of metallomesogens since these compounds can exhibit paramagnetism and/or mixed oxidation states properties key to the formation of magnetic and conductive materials, respectively.[3] Most bimetallomesogens reported in the literature consist of diamagnetic compounds.[4] However, only a few bimetallic complexes exhibit paramagnetic properties.[3,5]

In the present report we describe the synthesis and mesogenic properties of a group of binuclear paramagnetic complexes containing copper(II) and vanady(IV) metals derived from tetraimines obtained by condensation of mono-, di-, or tridecyloxy-4-benzoyloxy-2-hydroxybenzaldehyde and 3,3′,4,4′-biphenyltetraamine as shown in Scheme 1.

Results and Discusion

Synthesis and Characterization. The synthetic procedure for ligands and metal complexes is shown in Scheme 1. The Schiff bases were synthesized by literature procedures and were identified by ^{1}H NMR and elemental analysis.

The copper(II) and oxovanadium(IV) complexes were prepared by reacting the appropriate tetraimine with copper(II) acetate monohydrate or vanadyl(IV) sulfate pentahydrate in warm ethanol or methanol; the complexes were isolated as green or green-brown solids in good yields and were soluble in toluene, chloroform, and dichloromethane and insoluble in ethanol.

* To whom correspondence should be addressed. E-mail: joseluis@posta.unizar.es.

† Dedicated to Professor Domingo González, from the University of Zaragoza, on the occasion of his retirement.

(1) (a) Giroud-Godquin, A. M.; Maitlis, P. M. *Angew. Chem., Int. Ed. Engl.* **1991**, *30*, 375. (b) Espinet, P.; Esteruelas, M. A.; Oro, L. A.; Serrano, J. L.; Sola, E. *Coord. Chem. Rev.* **1992**, *117*, 215. (c) Serrano, J. L., Ed. *Metallomesogens: Synthesis, Properties and Aplications*; VCH: Weinheim, 1996. (d) Hudson, S. A.; Maitlis, P. M. *Chem. Rev.* **1993**, *93*, 861. (e) Bruce, D. W. In *Inorganic Materials*, 2nd ed.; Bruce, D. W., O'Hare, D., Eds.; Wiley: Chichester, 1996. (f) Collison, S. R.; Bruce, D. W. In *Transition Metals in Supramolecular Chemistry*; Sauvage, J. P., Ed.; Wiley: Chichester, 1999; Chapter 7.

(2) Lai, Ch., K.; Len, Y. F. *Liq. Cryst.* **1998**, *25*, 689.

(3) Lai, Ch., K.; Serrete, A. G.; Swager, T. M. *J. Am. Chem. Soc.* **1992**, *114*, 7948.

(4) (a) Espinet, P.; Etxebarria, J.; Marcos, M.; Pérez, J.; Remon, A.; Serrano, J. L. *Angew. Chem., Int. Ed. Engl.* **1989**, *28*, 1065. (b) Espinet, P.; Lalinde, E.; Marcos, M.; Perez, J.; Serrano, J. L. *Organometallics* **1990**, *9*, 555. (c) Barberá, J.; Espinet, P.; Lalinde, E.; Marcos, M.; Serrano, J. L. *Liq. Cryst.* **1987**, *2*, 833. (d) Baena, M. J.; Buey, J.; Espinet, A.; Kitzerov, H. S.; Heppke, G. *Angew. Chem., Int. Ed. Engl.* **1993**, *32*, 1201. (e) Eguchia, S.; Nozaki, T.; Miyasaka, H.; Matsumoto, N.; Okawa, H.; Kohata, S.; Hosino-Miyajima, N. *J. Chem. Soc., Dalton Trans.* **1996**, 1761. (f) Ghedini, M.; Pucci, D.; Munno, G. D.; Viterbo, D.; Neve, F.; Armentano, S. *Chem. Mater.* **1991**, *3*, 65. (g) Ghedini, M.; Longeri, M.; Bartolino, R. *Mol. Cryst. Liq. Cryst.* **1982**, *84*, 207. (h) Ghedini, M.; Licoccia, S.; Armentano, S.; Bartolino, R. *Mol. Cryst. Liq. Cryst.* **1984**, *108*, 269. (i) Ghedini, M.; Armentano, S.; Neve, F. *Inorg. Chim. Acta* **1987**, *134*, 23. (j) Eran, B. B.; Singer, D.; Praefke, K. *Eur. J. Inorg. Chem.* **2001**, 111, and references therein.

(5) (a) Pyzuk, W.; Krowcznsky, A.; Chen, L.; Gorecka, E.; Bickczantaev, I.; *Liq. Cryst.* **1995**, *19*, 575. (b) Lai, Ch. K.; Chen, F. G.; Ku, Y. J.; Tsai, Ch. H.; Lin, R. *J. Chem. Soc., Dalton Trans.* **1997**, 4683. (c) Lai, C. K.; Liu, R.; Kao, K. C. *J. Chem. Soc., Dalton, Trans.* **1998**, 1857. (d) Lai, C. K.; Len, Y. F. *Liq. Cryst.* **1998**, *25*, 689. (e) Kadkin, O.; Galiametdinov, Y.; Rakhmatullin, A. *Mol. Cryst. Liq. Cryst. Sci. Techol., Sect. A* **1999**, *332*, 2619. (f) Kadkin, O.; Galiametdinov, Y.; Rakhmatullin, A.; Mavrin, V. Y. *Russ. Chem. Bull.* **1999**, *48*, 379. (g) Ku, S. M.; Wu, Ch. Y.; Lai, C. K. *J. Chem. Soc., Dalton, Trans.* **2000**, 3491. (h) Binnemans, K.; Lodewyckx, K.; Donnio, B.; Guillon, D. *Chem. Eur. J.* **2002**, *8*, 1101.

10.1021/cm0209721 CCC: $25.00
Published on Web 01/25/2003

Scheme 1. Reagents and Conditions: (i) Dicyclohexylcarbodiimide (DCC), Dimethylaminopyridine (DMAP), Dichloromethane, r.t., 12 h; (ii) 3,3′,4,4′-Biphenyltetraamine, Toluene, *p*-Toluenesulfonic Acid (cat), Reflux, 12 h; (iii) Copper Acetate, Ethanol−Chloroform, Reflux, 1 h or Vanadyl Sulfate, Triethylamine, Methanol−Dichloromethane, Reflux, 1 h

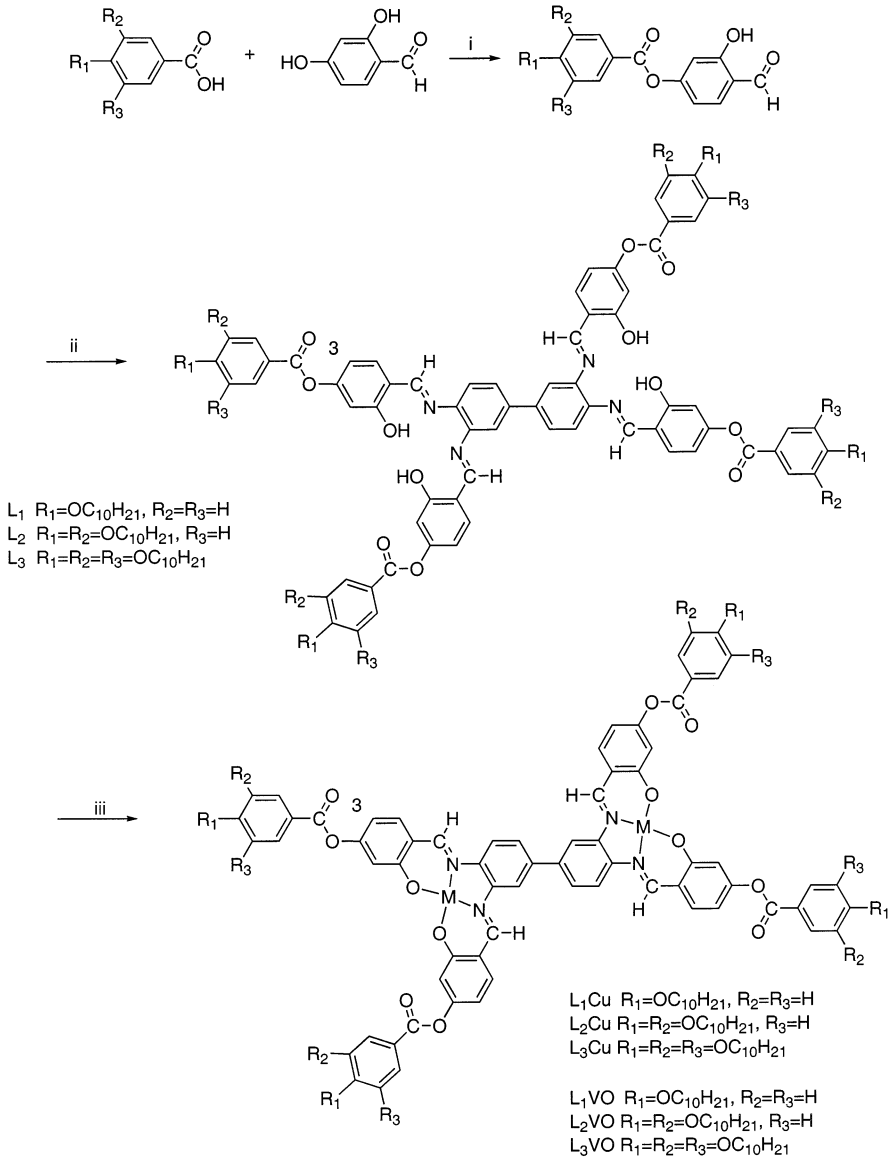

Table 1. Elemental Analysis for Imines and Complexes (Calculated Values in Parentheses), Molecular Weight, and Yields

compd	%C	%H	%N	MW	FAB$^+$	yield
L_3	72.5(72.6)	9.1(9.3)	1.9(1.8)	2986.3	2986	87
L_2	75.2(75.3)	8.6(8.8)	2.5(2.4)	2361.3	2362	89
L_1	74.8(74.6)	7.3(7.3)	3.4(3.2)	1736.2	1736	90
L_3Cu	72.4(72.6)	9.1(9.2)	1.9(1.9)	3109.4		82
L_2Cu	71.7(71.6)	8.2(8.2)	2.4(2.3)	2848.3		82
L_1Cu	70.0(69.8)	6.5(6.6)	3.1(3.0)	1859.3	1882 $[M + Na]^+$	87
L_3VO	72.3(72.5)	9.1(9.1)	1.9(1.8)	3116		79
L_2VO	71.5(71.4)	8.1(8.2)	2.1(2.3)	2491	2490 $[M - 1]$	82
L_1VO	69.5(69.5)	6.8(6.6)	3.0(3.0)	1866	1889 $[M + Na]^+$	85

Elemental analysis of ligands and complexes are consistent with the proposed structures, confirming the bimetallic composition of the complexes (Table 1). The infrared spectra of the metallic complex shows a stretching band around 1609 cm^{-1}, which is assigned to ν(C═N); it is found that this band shifts to a lower frequency by ca. 5−9 cm^{-1} compared to that of the free Schiff bases. The vanadyl complexes also exhibit a stretching band at ca. 981 cm^{-1} of V═O bonding, indicating a monomeric structure.

Mesomorphic Behavior. All the ligands and their metal complexes exhibit liquid-crystalline behavior, which was studied by polarized optical microscopy, DSC and X-ray diffraction. The thermal data are summarized in Table 2.

The DSC thermograms do not show transitions of measurable enthalpy and particularly second scan cycles do not display any transition peak. This is probably due to slow crystallization or vitrification of the mesophases, which is seen at the microscope like a freezing of the texture.

Ligands L_3 and L_2 exhibit similar behavior. On cooling from the isotropic liquid, a fluid birefringent texture is displayed with homeotropic domains after shearing. This is attributed to a hexagonal columnar mesophase that was confirmed by XRD. The ligand L_3 with a higher number of terminal chains displays lower transition temperatures than L_2.

Table 2. Phase Behavior of Ligand and Copper(II) and Vanadium(IV) Complexes

compd	phase[a–c]
L_3	g 36 Col_h 132 I
L_2	g 102 Col_h 208 I
L_1	Cr 189 SmC 200 I
L_3Cu	g 165 Col_h 202 I
L_2Cu	g 189 Col_h 297 I dec.
L_1Cu	Cr 190 SmC 230 I dec.
L_3VO	g 140 Col_h 187 I
L_2VO	g 120 Col_h 238 I dec.
L_1VO	Cr 215 SmC 293 dec.

[a] g = frozen mesophase, Cr = crystal phase, Col_h columnar hexagonal mesophase, SmC = smectic C mesophase, and I = isotropic liquid. [b] Transition temperatures (°C). [c] Optical data.

Compound L_1 with four terminal chains exhibit a smectic C mesophase characterized by blurred and schlieren textures. All the ligands decompose in the isotropic liquid at temperatures higher than 215 °C.

Metal complexes display mesomorphic behavior similar to the ligands but with higher transition temperatures. Due to the complexation, the ligand becomes rigidified, loses degrees of motional freedom, and therefore organizes much more efficiently; hence, the transition temperatures increase.

Copper and oxovanadium complexes derived from ligands L_3 and L_2 exhibit columnar hexagonal mesophases and complexes derived from L_1 display smectic C mesophases. In all cases the textures are akin to the ones displayed by the ligands. Again, we observe a decrease of the clearing temperatures when the number of chains increases.

This similar behavior of ligands and complexes is explained by the fact that the structure of the ligand does not change in terms of size or shape when complexed to the metals.

X-ray Diffraction Study. The mesophases of these compounds were studied by X-ray diffraction and in all cases the patterns supported the nature of the mesophases assigned on the basis of the microscope textures.

X-ray patterns were taken at high temperatures. However, in most of the cases it was observed that the mesophases freeze at room temperature and remain as such for long periods of time (L_2 and L_3 and derived complexes) or for a limited period before recrystallizing (L_1 and derived complexes). Therefore, room-temperature patterns were also taken on the frozen mesophases. Moreover, the X-ray photographs taken on some virgin samples were also characteristic of a liquid-crystal phase.

L_3 and Its Complexes. The as-obtained compound L_3 is a solid at room temperature. However, the X-ray patterns taken on a virgin sample of this compound is typical of a liquid-crystal phase. The X-ray photographs were also registered at 110 °C, a value above the temperature at which the mesophase becomes a fluid. In both cases, a set of three or four sharp reflections are observed in the small-angle region of the pattern with a reciprocal spacing ratio of $1:\sqrt{3}:\sqrt{4}(:\sqrt{7})$. These reflections are more clearly visible in the patterns taken at room temperature on a sample cooled from the fluid mesophase, and the reciprocal ratio obtained is characteristic of a two-dimensional hexagonal structure. The spots are indexed, respectively, as the (1 0), (1 1), (2 0), and (2 1) reflections from the two-dimensional (2-D) lattice and this confirms that the mesophase of this compound is columnar hexagonal (Col_h), as suggested by the textures observed in the polarizing microscope. The hexagonal lattice constant *a* deduced from the measured reflections is 46 Å at room temperature and 44 Å at 110 °C. The decrease of the constant upon increasing the temperature is consistent with the higher conformational freedom of the hydrocarbon chains, which reduces the effective molecular diameter. It is concluded that this compound is mesomorphic in the entire temperature range studied, and the fluid mesophase freezes below the glass transition (36 °C) to yield a mesomorphic glass.

The behavior of compounds L_3Cu and L_3VO is similar to that of their precursor ligand L_3. The X-ray photographs taken at room temperature on these compounds are characteristic of a liquid-crystal phase. The patterns are consistent with a frozen hexagonal columnar mesophase, and the measured lattice constant *a* is 44 Å for L_3Cu and 45 Å (43 Å after cooling from the fluid mesophase) for L_3VO. X-ray photographs were also taken at high temperatures, and the measured hexagonal lattice constant *a* is 42 Å at 180 °C for L_3Cu and 43 Å at 170 °C for L_3VO.

In addition to the above-mentioned features, the X-ray photographs of the three compounds (L_3 and its two complexes) show a diffuse halo at large angles that corresponds to a distance of about 4.5 Å. This scattering is classically observed for any liquid-crystal phase and is characteristic of the interferences between the conformationally disordered hydrocarbon chains.

L_2 and Its Complexes. The results of the X-ray study for L_2 and L_2VO are similar to the results for L_3 and its complexes. Their X-ray patterns are consistent with a hexagonal columnar mesomorphic glass at room temperature both for virgin and for thermally treated (cooled from the fluid mesophase) samples. On the other hand, the copper complex L_2Cu is partially crystalline, and the high temperature at which it becomes fluid prevented the study of its mesophase with our X-ray setup. The measured lattice constant *a* measured at room temperature is 51 Å (49 Å after thermal treatment) for L_2 and 50 Å (49 Å after thermal treatment) for L_2VO. At 140 °C the measured hexagonal lattice constant *a* is 48 Å for L_2 and 47 Å for L_2VO.

In the large-angle region of the X-ray photographs taken on these compounds at room temperature, in addition to the halo characteristic of the hydrocarbon chains, an outer diffuse halo is found that corresponds to a distance of about 3.5 Å. This scattering is not observed in L_3 and its complexes and is probably related to the stacking spacing.

It is intereresting to note that the hexagonal lattice constants are larger for these compounds that contain two hydrocarbon chains per ring than for the analogues with three chains per ring (and hence with higher molecular mass). A decrease in the lattice constant (and hence an increase in the mean stacking distance) upon increasing the number of peripheral chains has also been observed for other columnar liquid crystals[6] and

(6) (a) Barberá, J.; Esteruelas, M. A.; Levelut, A. M.; Oro, L. A.; Serrano, J. L.; Sola, E. *Inorg. Chem*. **1992**, *31*, 732. (b) Barberá, J.; Elduque, A.; Giménez, R.; Lahoz, F. J.; López, J. A.; Oro, L. A.; Serrano, J. L.; Sola, E.; *Inorg. Chem*. **1998**, *37*, 2960.

is a consequence of the greater spacial requirements of the chains out of the molecular plane.

L_1 and Its Complexes. According to the textures observed in the polarizing microscope, these compounds show smectic C mesomorphism. This was supported by the X-ray patterns taken at high temperatures on L_1 and L_1Cu. The patterns contain a single sharp maximum at small angles due to the reflection of the X-rays on the smectic layers, and some diffuse scattering at large angles, related to the conformationally disordered chains. On the other hand, the high temperature at which the solid vanadium complex melts into the mesophase prevented its study with our X-ray diffractometer. In the case of the organic compound and the copper complex, the mesophase can be partially frozen by quickly cooling to room temperature, although the X-ray patterns revealed that it coexists with some crystalline phase. Both at room and at high temperature, the small-angle sharp ring gives the layer spacing in the smectic structure. The measured value of this parameter is 39 Å at 170 °C (measured in the cooling process) and 42 Å at room temperature for L_1, and 44 Å at 192 °C and 47 Å at room temperature for L_1Cu. These values are consistent with a rather elongated molecular conformation, but with a greater tilt angle in the organic compound than in the copper complex.

EPR Study. Copper and vanadyl complexes derived from L_3, L_2, and L_1 are paramagnetic. It is known that EPR spectra of metallomesogens are affected by the structure and dynamics of the mesophase.[7] It is interesting to study complexes containing similar metal centers but reaching different mesophases, in order to reveal the effect of the ordering on the EPR signal and to obtain information about molecular arrangement and dynamics. With this aim, X-band EPR spectra of powder samples of the copper and vanadyl complexes derived from L_2 and L_1 compounds were taken at different temperatures between room temperature and 235 °C. Our EPR results for each complex will be presented and analyzed separately.

L_2VO Complex. The compound at room temperature shows an EPR spectrum typical for this kind of compound that corresponds to a vanadyl center in a square pyramidal environment (Figure 1A). The spectra can be interpreted using a spin Hamiltonian with a Zeeman and a hyperfine term (arising from the interaction between the electronic spin and the ^{51}V nuclear spin).[7]

Both terms are approximately axial with the following hyperfine (**A**) and gyromagnetic (**g**) parameters:

$$A_{\parallel} = 486 \pm 3 \text{ MHz} \qquad A_{\perp} = 174 \pm 3 \text{ MHz}$$

$$g_{\parallel} = 1.953 \pm 0.003 \qquad g_{\perp} = 1.980 \pm 0.003$$

When the temperature increases, small but detectable changes in the hyperfine parameters take place (see Figure 1B). Near to the melting point, hyperfine parameters start to change: $A_{\parallel}$ decreases as the temperature increases, whereas $A_{\perp}$ increases. This effect is more noticeable for the parallel parameter: at 217 °C $A_{\parallel} = 473$ MHz ($\Delta A_{\parallel} = 12$ MHz, from the RT value) and $A_{\perp} = 183$ MHz ($\Delta A_{\perp} = 6$ MHz).

(7) . Alonso, P. J. In *Metallomesogens*; Serrano, J. L., Ed.; VCH: Weinheim, 1996; Chapter 9.

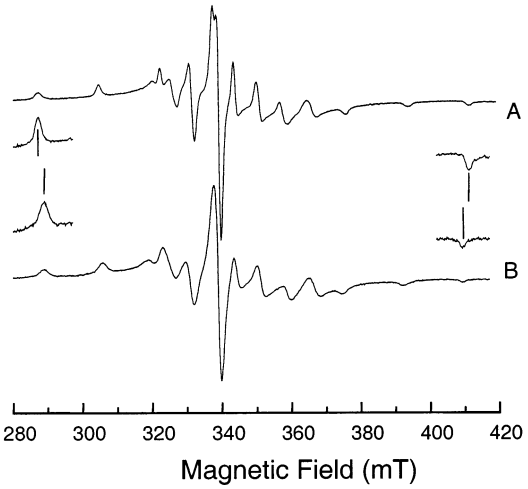

Figure 1. X-band EPR spectra of powder samples of the L_2-VO compound. A, room temperature; B, 217 °C. Detail of outermost peaks of the parallel feature shows the dynamical shifting (see text).

These changes of the measured hyperfine coupling in the mesophases are due to a dynamic process.[7] When a paramagnetic center reorients in a fast and isotropic way, the anisotropy of the **g** and **A** tensors is averaged to zero and both $A_{\parallel}$ and $A_{\perp}$ parameters reach the same (isotropic) value. Partial averaging of the hyperfine anisotropy takes place for the cases of slow or nonisotropic tumbling. For slow motion, an additional motional broadening occurs.

Molecules in columnar mesophases show anisotropic tumbling because of the movement restrictions imposed by the phase structure. When the reorientations are fast as compared to the averaged frequency, the value of the "effective" (measured) parameters do not depend on the motion rate and can give information about the molecular order in the mesophase. In our case, considering the molecule as a rigid disk, the reorientation of the molecular axis can partially average the anisotropy of the hyperfine coupling. Given that this kind of motion has a typical frequency larger than 10^7-10^8 s^{-1}, and that the EPR spectra of the mesophase do not seem to show a noticeable motional broadening, it is likely that the effect of this reorientation on the hyperfine coupling corresponds to the fast motion regime. Thus, the measured parallel hyperfine coupling is related to an "order parameter" (let us call it P) of the molecule within the columns:

$$(A_{\parallel})_{\text{eff}} = A_{\text{iso}} + 2P(A_{\parallel} - A_{\perp})/3$$

where

$$A_{\text{iso}} = (A_{\parallel} + 2A_{\perp})/3$$

Similarly,

$$(A_{\perp})_{\text{eff}} = A_{\text{iso}} - P(A_{\parallel} - A_{\perp})/3$$

Other motional modes could in principle affect the measured hyperfine parameters. Torsion of the molecule around the central phenyl−phenyl bond would cause additional averaging that would not depend on the order parameter. However, the effect of this mode on our measured hyperfine parameters must be very small

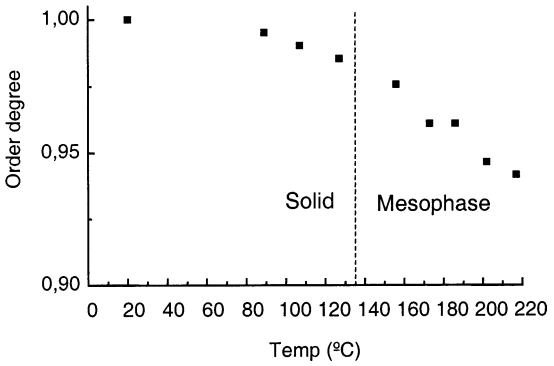

Figure 2. Thermal evolution of the *P* parameter of L_2VO (see text).

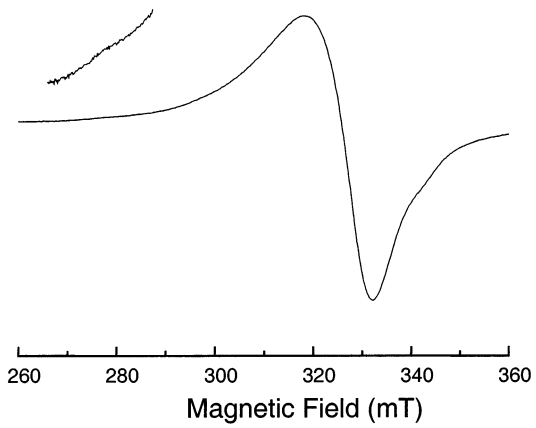

Figure 3. X-band EPR spectra of a L_2Cu powder sample at room temperature. Detail shows the broad shoulder at low magnetic field (see text).

because such motion would average the hyperfine tensor in a way that would break its axial symmetry and would increase one of the measured "perpendicular" parameters by the same quantity that the parallel one decreases. This behavior is not observed in our spectra.

So we can estimate the order parameter *P* from our EPR spectra. Its thermal evolution is seen in Figure 2. The order is very high in the region measurable by EPR (temperature below 230 °C). This fact is related to the compact molecular packing within the column. Although the obtained parameter *P* is not an actual order parameter (because it does not reflect the order of the different columns), it is worth noting that it is obtained measuring the motion of the molecules that forms the mesophase and not that and the external probe.

L_2Cu Complex. The EPR signal measured in the powder sample at room temperature (Figure 3) shows a very broad, asymmetric feature centered at $g_{eff} \approx 2.07$. A shoulder at a magnetic field of about 272 mT can also be distinguished. The signal can be interpreted as being due to Cu^{2+} centers in a square planar environment.[7] The parallel hyperfine structure is not resolved because of the line width.

There are several factors that can cause such large signal broadening in this kind of compound (dipole−dipole magnetic interactions, inhomogeneous distribution of copper environments,[8] and weak magnetic exchange interaction[9]), but their relative contributions cannot be separated.

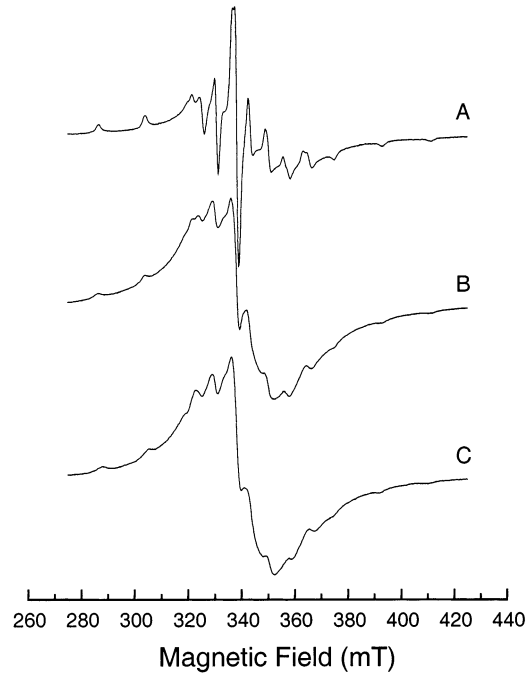

Figure 4. X-band EPR spectra of L_1VO. A, room temperature, virgin sample; B, room temperature, after a first heating to above the melting point and a cooling; C, 220 °C (S_c phase).

The EPR spectrum only shows a slight broadening as the temperature is increased in the solid and liquid-crystal phases.

L_1VO Complex. The powder sample of the virgin compound at room temperature displays a signal very similar to L_2VO (Figure 4A), which can be interpreted in the same way. When the melting point is reached on the first heating cycle, the signal undergoes significant broadening, and after cooling this broad signal is displayed over the whole range of temperatures measured (Figure 4B,C). This effect is not detected in L_2-VO spectra. This is related to the change from a crystalline structure to a smectic glass at room temperature after the first process of heating above the melting point and cooling. Given that the EPR signal width of these compounds is mainly driven by intermolecular spin interactions, the molecular rearrangement causes significant changes in the appearance of the EPR signal.

The EPR signal of this compound is clearly different from the one of L_2VO. It can be interpreted by the same spin Hamiltonian parameter, but with a much higher line width. This is related to the different kinds of liquid-crystal phases each material can exhibit. Molecules of L_1VO adopt a compact smectic arrangement that results in a broader EPR signal. Other differences are also noticeable when the thermal evolution of the EPR spectra are compared. Following the thermal evolution of the two outermost parallel peaks, it is seen that a small reduction in their distance occurs in the solid phase. It is due to small libration motion because of the thermal expansion. On the other hand, no change of the distance is detected at the temperatures in the SmC mesophase. The mesophase retains a compact molecular arrangement and no mesurable effect of molecule reorientation appears.

(8) Martínez, J. I.; Marcos, M.; Serrano, J. L.; Orera, V. M.; Alonso, P. J. *Liq. Cryst.* **1995**, *19* (5), 603.

(9) . Barberá, J.; Marcos, M.; Omenat, A.; Serrano, J. L.; Martínez, J. I.; Alonso, P. J. *Liq. Cryst.* **2000**, *27* (2), 255.

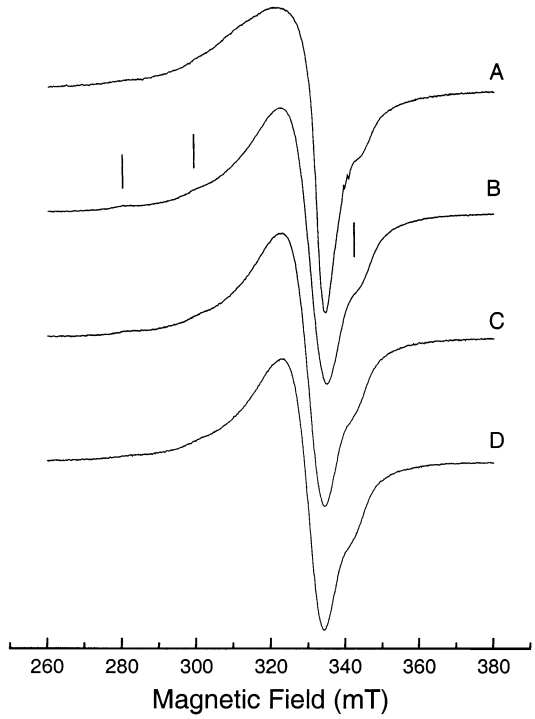

Figure 5. X-band EPR spectra of L_1Cu. A, room temperature, virgin sample; B, room temperature, after a first heating to above the melting point and a cooling (sticks are showing the detected *parallel* features); C, 210 °C (SmC phase); D, 235 °C (isotropic liquid phase).

L_1Cu Complex. The EPR spectrum of the freshly prepared sample at RT is very similar to the one measured for L_2Cu and can be interpreted in the same way (Figure 5A). As for its VO counterpart, the spectra displayed after the first heating show changes associated with a different signal width (Figure 5B) and are related to a different molecular arrangement. The signal shows features narrow enough to display three of the four *parallel* peaks resolved. Thus, the spin Hamiltonian parameters can be determined more accurately:

$$A_{\parallel} = 570 \pm 10 \text{ MHz} \qquad A_{\perp} < 30 \text{ MHz}$$

$$g_{\parallel} = 2.21 \pm 0.01 \qquad g_{\perp} \approx 2.06$$

The EPR spectra measured at different temperatures between room temperature and 235 °C (above the clearing point) show no changes in these parameters, within the error values (Figure 5B,C,D). As in the case of L_1VO, this indicates that molecules in the SmC mesophase are enclosed in a compact packing and its reorientation is severely reduced. Even in the isotropic liquid phase, where the global orientational order vanishes, our results indicate that these large molecules preserve a quite compact local arrangement.

The liquid-crystal glass of L_1Cu appears to display an EPR signal narrower than the corresponding L_2Cu one at room temperature. The opposite occurs for the vanadyl complexes. The effect of intermolecular magnetic exchange interaction, which usually takes place in this kind of Cu complex but not in the VO ones, could account for the difference. In our case, all the spectra of Cu compounds show a parallel hyperfine parameter that is only compatible with a weak exchange interaction. Then the exchange should cause a broadening of the signal width. The line width difference could be due to some weak exchange taking place in the L_2Cu compound that were not important in L_1Cu. It is worth noting that intermolecular exchange depends not only on distance but also on the disposition of the adjacent molecules. Thus, smectic local arrangement of L_1Cu could be more compact but less appropriate to allow an "exchange path" between molecules.

Another possibility for explaining the different line width could be that the compact smectic arrangement causes a more homogeneous environment for the copper centers when compared with the discotic arrangement, reducing the inhomogeneous distribution of spin Hamiltonian parameters and therefore displaying narrower EPR signals. These two effects cannot be distinguished from our experimental evidence.

Conclusions

Free ligands L_2 and L_3 exhibit a hexagonal columnar mesophase in the entire temperature range studied below the clearing point. The mesophase is fluid above the glass transition and freezes below that temperature to yield a mesomorphic glass. Their metal-containing derivatives behave like the precursory ligands.

Ligand L_1 and its complexes are crystalline in the virgin state and melt into a fluid smectic C mesophase that, at least for L_1 and L_1Cu, can be frozen upon cooling back to room temperature.

L_2 and L_1 copper and vanadyl complexes show different EPR signal behaviors that have been interpreted on the basis of the different effects of columnar and smectic phase arrangement. In the case of L_2VO compound, an estimation of the molecular order within the columns of the mesophase has been obtained from EPR measurements.

Experimental Section

All chemicals for synthesis were reagent grade from Aldrich Chemical Co. and used without further purification. Solvents were purified and dried by standard techniques.

The synthetic procedure leading to the target complexes is outlined in Scheme 1.

The free ligands were synthesized by using well-known methods by condensing the appropriate mono-, di-, or tridecyloxy-4-benzoyloxy-2-hydroxybenzaldehyde with the 3,3′,4,4′-biphenyltetraamine in toluene using a Dean−Stark apparatus.

L_3. ^{1}H NMR (300 MHz, $CDCl_3$), δ (ppm): 0.83−0.87 (m, 36H), 1.25−1.84 (m, 192H), 4.03 (t, 24H), 6.81 (d, J = 8.0 Hz,-4H), 6.89 (d, 2.2 Hz, 4H), 7.38 (s, 8H), 7.44−7.55 (m, 6H), 7.63 (d, J = 9.7 Hz, 4H), 8.72 (s, 2H), 8.74 (s, 2H), 13.29 (s, 2H), 13.35 (2s, 2H). IR (Nujol) ν (cm^{-1}): 1734, 1618. Elemental analysis and molecular weight are collected in Table 1.

L_2. ^{1}H NMR (300 MHz, $CDCl_3$), δ (ppm): 0.88 (m, 24H), 1.28−1.85 (m, 128H) 4.07 (t, 16H), 6.84 (d, J = 8.0 Hz, 4H), 6.92 (s, 4H), 6.93 (d, J = 8.0 Hz, 4H), 7.37−7.50 (m, 10H), 7.66 (s, 4H), 7.81 (d, J = 8.0 Hz, 4H), 8.73 (s, 2H), 8.76 (s, 2H), 13.29 (s, 2H), 13.35 (2s, 2H). IR (Nujol) ν (cm^{-1}): 1730, 1618. Elemental analysis and molecular weight are collected in Table 1.

L_1. ^{1}H NMR (300 MHz, $CDCl_3$), δ (ppm): 0.87 (m, 12H), 1.26−1.83 (m, 64H) 4.03 (t, 8H), 6.80−6.91 (m, 8H), 6.95 (d, J = 8.8 Hz, 8H), 7.34−763 (m, 10H), 8.11 (d, J = 8.8 Hz, 8H), 8.69 (s, 2H), 8.73 (s, 2h), 13.28 (s, 2H), 13.33 (2s, 2H). IR (Nujol) ν (cm^{-1}): 1728, 1618. Elemental analysis and molecular weight are collected in Table 1.

Preparation of the Complexes. The copper(II) complexes were prepared by the addition of an ethanolic solution (20 mL)

containing copper acetate ($Cu(OAc)_2 \cdot H_2O$) (2 mmol) to a hot solution of the appropriate imine (1 mmol) in a mixture of chloroform-ethanol (100 mL). The solution was heated under reflux for 1 h. After cooling, the precipitate was collected by filtration and recrystallized from ethyl acetate.

Elemental analysis, yields, and molecular weight are collected in Table 1.

The oxovanadium(IV) complexes were prepared by the addition of a methanolic solution (20 mL) containing vanadyl sulfate ($VOSO_4 \cdot 5H_2O$) (2 mmol) to a hot solution of the appropriate imine (1 mmol) and triethylamine (4 mmol) in a mixture of dichloromethane−methanol (100 mL). The solution was refluxed for 1 h. After cooling, the precipitate was collected by filtration and recrystallized from ethyl acetate.

Elemental analysis, yields, and molecular weight are collected in Table 1.

Techniques. Microanalysis was performed with a Perkin-Elmer 240 B microanalyzer. Infrared spectra were obtained by using a Perkin-Elmer 1600 (FTIR) spectrophotometer in the 400−4000-cm^{-1} spectral range. ^1H NMR spectra were recorded on a Varian Unity 300-MHz spectrometer in $CDCl_3$ solutions.

The optical textures of the mesophases were studied with a Nikon polarizing microscope equipped with a Mettler FP8 hot stage and a FP80 central processor. The transition temperatures and enthalpies were determined by differential scanning calorimetry with a Pekin-Elmer DSC-7 instrument operated at a scanning rate of 10 °C/min on heating. The apparatus was calibrated with indium (156.6 °C, 28.4 J/g) as the standard. X-ray diffraction experiments were carried out on powder samples with a pinhole camera (Anton-Paar) operating with a point-focused Ni-filtered Cu Kα beam. The samples were held in Lindemann glass capillaries (1-mm diameter) and heated, when necessary, with a high-temperature attachment. The X-ray patterns were collected on a flat photographic film.

EPR measurements at X-band (microwave frequency about 9.6 GHz) were taken with a Bruker ESP380 spectrometer. The Bruker ER4111VT variable temperature accessory was used for measurements above room temperature.

Acknowledgment. This work was supported by the CICYT (Spain) (Projects MAT99-1009-CO2-02 and MAT2000-1293-CO2-01).

CM0209721